Intracranial fluid dynamics changes in idiopathic intracranial hypertension: pre and post therapy

Agarwal N.[1,2,3], Contarino C.[4], Bertazzi L.[5], N. Limbucci[6], Toro E. F.[7]

[1] *Section of Radiology, Hospital Santa Maria del Carmine, Rovereto, TN, Italy*

[2] *Center for Mind/Brain Sciences CIMeC, University of Trento, TN, Italy*

[3] *Section of Neuroradiology, Department of Radiology and Imaging Sciences, University of Utah, USA*

[4] *Department of Mathematics, University of Trento, Trento, TN, Italy*

[5] *Section of Ophthalmology, Ospedale Santa Maria del Carmine, Rovereto, TN, Italy*

[6] *Neurovascular Interventional Unit, Careggi University Hospital, Florence, Italy*

[7] *Laboratory of Applied Mathematics, University of Trento, Trento, TN, Italy*

Corresponding author:

Nivedita Agarwal

Santa Maria del Carmine Hospital

Azienda Provinciale per i Servizi Sanitari

Corso Verona, 4

38068, Rovereto (TN), Italy

Tel: +39 - 0464 404066

Email: niveditaaga@gmail.com

Keywords:

Idiopathic intracranial hypertension, Cerebrospinal fluid, Phase contrast-cine magnetic resonance imaging, dural venous stenosis, papilledema

Running title: MR fluid analysis in IIH

Abbreviations: AaCD=artero-aqueduct CSF delay; AcCD= artero-cervical CSF delay; aCSF=CSF through the AoS; AoS=aqueduct of Sylvius; AVD=arterovenous delay; CC= cardiac cycle; cCSF=CSF in the cervical subarachnoid space; CSF=cerebrospinal fluid; CVO=cerebral venous outflow; ICA=internal carotid artery; ICP = intracranial pressure; IIH = idiopathic intracranial hypertension; IJV=internal jugular vein; tA=total cerebral arterial inflow; tIJV=total outflow from internal jugular veins; LP=lumbar puncture; RFNL = retinal fiber nerve layer; PCC-MR=phase contrast cine magnetic resonance; SAS=subarachnoid space; TS=transverse sinus; VA= vertebral artery

Abstract

Idiopathic intracranial hypertension (IIH) is a condition of unknown etiology frequently associated with dural sinus stenosis. There is emerging evidence that venous sinus stenting is an effective treatment. We use phase contrast cine MRI to observe changes in flow dynamics of multiple intracranial fluids and their response to different treatments in a patient with IIH. We quantified the following parameters at the level of the aqueduct of Sylvius and the cervical C2C3: cerebrospinal fluid (CSF), arterial and venous flow; CSF velocity amplitude; artero-venous delay (AVD); artero-CSF delay and percentage of venous outflow normalized to total arterial inflow (tIJV/tA). Analyses were run before lumbar puncture (LP) (A), after LP (B), after medical therapy (C) and after venous stent placements deployed at two separate times (D and E). AVD and tIJV/tA improved only after CSF removal and after stent placements. CSF velocity amplitude remained elevated. Arterial flow profile showed a dramatic reduction after LP with improvement in mean venous flow. This report is the first to demonstrate interactive changes in intracranial fluid dynamics that occur before and after different therapeutic interventions in IIH. We discuss how increased intracranial venous blood could be “tumoral” in IIH and facilitating its outflow could be therapeutic.

Introduction:

Idiopathic intracranial hypertension (IIH) is a neurological condition of unknown etiology, which requires prompt diagnosis and if left untreated could result in rapid progressive visual loss (Mollan *et al.*, 2016). A high opening cerebrospinal fluid (CSF) pressure during lumbar puncture (LP) is indicative of increased intracranial pressure (ICP). Increased CSF opening pressure coupled with normal neuroimaging findings are generally sufficient to make a definite diagnosis of IIH in obese females of childbearing age (Friedman *et al.*, 2013). Periodic removal of CSF through LP or the use of CSF diversion procedures are widely accepted therapeutic interventions to reduce ICP in these patients. Adjunct medical therapy consists of the use of carbonic anhydrase inhibitors or topiramate and shows little success.

Intracranial volume is maintained constant (Monroe-Kellie) in a rigid skull encasement, during each cardiac cycle (CC), through a complex temporal synchronization of multicompartment intra and extracranial fluid dynamics (Beggs *et al.*, 2013). How increased CSF pressure in the subarachnoid space (SAS) influences intracranial arterial and venous fluid dynamics within the framework of the Monroe-Kellie hypothesis remains unclear. Bateman showed that in IIH, the total cerebral arterial inflow is increased by 21% and the correspondent percentage of venous outflow through superior sagittal sinus (SSS) is reduced (Bateman, 2008b). On the venous front, there is evidence that almost 93% of patients with IIH harbor some degree of dural sinus stenosis (Morris *et al.*, 2017). Stenosis can be intrinsic or extrinsic, dynamic or static. While still debatable, there is growing

evidence that CSF removal during LP causes transient resolution of dural venous sinus stenosis, suggesting that these are more likely extrinsic (Buell *et al.*, 2017; Juhász *et al.*, 2017; Rohr *et al.*, 2007). The increased resistance to venous outflow will further augment CSF pressure in the SAS by obstructing its absorption at the level of arachnoid granulations, thus leading to a vicious cycle. Improvement of venous outflow by use of stents can facilitate venous outflow and CSF absorption (Aguilar-Pérez *et al.*, 2017; R. I. Farb *et al.*, 2003).

Phase contrast cine MR (PCC-MR) is a consolidated non-invasive technique often employed in clinical settings to allow quantification of CSF flow parameters in the aqueduct of Sylvius (AoS) and determine therapeutic strategies (Stoquart-El Sankari *et al.*, 2008; Yousef *et al.*, 2016). It can provide useful information regarding velocity, flow, amplitude and direction of CSF flow but also in the arteries and veins (Enzmann and Pelc, 1993; Lagana *et al.*, 2014).

In this study, we set to observe changes in the temporal coupling and dynamics of arterial, venous and CSF compartments using PCC-MR in a patient with IIH. We repeated these analyses at different time points. The results were compared with data acquired on a healthy subject and with reported values in the literature.

Methods:

A 34 yr old obese female reported multiple episodes of neck pain, throbbing headache and progressive vision loss. LP was performed in a seated position

and the opening CSF pressure was read using a hand held manometer attached to the needle. Visual acuity was assessed through Snellen charts. Visual field (VF) pattern was studied by standard automated perimetry and retinal fiber nerve layer (RFNL) thickness was measured using optical coherence tomography (OCT). Standard venous digital angiography was performed and venous pressure was measured at various locations by attaching a pressure transducer to the microcatheter.

MRI acquisition: secondary causes were ruled out using standard diagnostic sequences (T1-SE, T2-TSE, FLAIR, DWI) using a 1.5 Tesla MR scanner (Siemens, Erlangen, Germany). Gadolinium-based venography (MRV) was performed to study venous sinus anatomy. Flow study was performed using a retrospective pulse-gated gradient echo sequence with a TR/TE of 22.9/7.0 ms. The 2D single 5mm slice of the PC sequence was positioned orthogonal to the direction of flow at the AoS (aCSF) and in the anterior CSF space between the C2 and the C3 vertebral level (cCSF) with a VENC of 20/50cm/s (CSF/vessels). 40 phases were acquired corresponding to one CC. Cardiac triggering was performed prospectively with finger plethysmography. The same protocol was run before LP (A), after 7 hours of LP (B) and after two months of standard medical treatment (C). The protocol was repeated after one month of venous stent placement in the transverse sinus (TS) (D) and again after one month of stent placement in the right TS (E). All acquisitions were performed by the same neuroradiologist. The same protocol was collected on a healthy 26 yr old male.

Four fluid compartment analysis: CSF and blood flow quantifications were performed using SPIN (Signal Processing in NMR, Detroit, MI). Post-processing was done using MATLAB (The MathWorks, Natick, MA). Flow and velocity profiles were smoothed using built-in functions of MATLAB. A region of interest (ROI) was manually drawn for each vessel in the magnitude images of the PCC. Over the CC, the size, shape and location of each ROI were kept fixed. At C2C3 level we manually drew 7 ROIs: left/right internal jugular veins (IJVs), internal carotid arteries (ICAs), vertebral arteries (VAs) and one additional ROI for the phase offset (supplementary Fig. 1). For CSF (aCSF and cCSF), we manually drew a ROI on the phase image corresponding to the highest caudal velocity and one additional ROI for the phase offset. The cross-sectional area of the ROI was assumed to remain constant across all time points. Velocity amplitude of the aCSF and the cCSF was calculated from the maximum and minimum peaks of their absolute values. Arteriovenous delay (AVD) was estimated as the lag in time between arterial and venous systolic peaks and was represented as a percentage of CC. Artero-CSF delays were estimated as the lag in time between arterial systolic peak and aCSF (AaCD) and cCSF (AcCD). To assess the contribution of collateral pathways for venous blood flow exiting the intracranial compartment, we calculated the ratio, expressed in percentage, between the total internal jugular vein outflow (tIJV) and the total intracranial arterial inflow (tA), that is tIJV/tA=tIJV/(ICAs+VAs) (Lagana *et al.*, 2014). When tIJV/tA is close to 100%, venous blood outflow through the IJVs matches the arterial blood inflow, and therefore the contribution of collaterals is

minimum. On the contrary, when tIJV/tA decreases to zero, major contribution is given by collateral pathways (Doepp *et al.*, 2004).

Results

I) Pretreatment data (A)

Clinical status: neurological exam was normal. Opening LP pressure was 50 cmH_20 (normal value in the seated position is <34.6 cmH_20) (Abualenain *et al.*, 2011) that dropped to 24cmH_20 after removing 30mL of CSF. *Ophthalmologic findings:* visual acuity was reduced in both eyes (right eye 20/100, left eye 20/25). Severe bilateral papilledema was noted with slit-lamp examination. *MRI and MRV:* MRI was negative for space occupying disease. Enlarged optic nerve sheaths were found bilaterally: 7.2mm on the right side and 8.4mm on the left side (normal values are 5.2 ± 0.9 mm) (Passi *et al.*, 2013). 3D MRV showed a left TS stenosis. *Angiographic procedure*: bilateral stenosis at the transverse-sigmoid sinus junction was observed with pressure difference of 4 mm Hg across the left TS and only 1 mmHg across the right TS. Only the left TS was stented by placing a 7x50 mm Carotid Wallstent that lowered the difference to 1 mmHg (D) (Supplementary Fig. 2).

PCC-MRI: The temporal order of all four systolic peak flows was conserved in the patient with respect to both our healthy subject and that reported in the literature (Fig. 1a) (Beggs, 2014). The AVD was 15.35% of CC and in the normal range (Table 1). Likewise, the AaCD and AcCD were also in the normal range (20.74% and 5.35% respectively) (Table 2). aCSF velocity amplitude in the patient was almost three times higher than that of healthy

subject (12.24cm/s vs. 4.15cm/s) (Supplementary figure 3). cCSF caudal peak velocity and flow were within the normal range (-2.93cm/s and -2.96mL/s respectively) (Table 2). While mean arterial flow was in the normal range (13.35mL/s), the systolic peak showed a longer plateau (Fig. 2A). Mean venous flow, in absolute value, was below normal minimum values (5.88mL/s) (Table 1). The tIJV/tA was 44% with respect to 93.5% in the healthy subject.

II) Post-treatment data (B, C, D and E)

Clinical status: no clinical improvement was noticed by the patient at B and at C. Mild relief in headache was referred at time point D but immediate benefit was reported after time point E. *Ophthalmologic findings:* there was a trend towards progressive decrease in visual function at time points B and C whereas at time points D and E all visual function including RNFL parameters appeared stable in both eyes with slight visual improvement in the left eye (data not shown). *MRI and MRV:* no morphologic changes were observed at any time point except a 1 mm reduction in the left optic nerve sheath diameter at E. MRV did not change at B and C. At D, the right TS was severely reduced in diameter. *Angiographic procedure:* two months after D, a new right TS stenosis with a pressure difference of 6 mm Hg difference was found and a second stent was deployed (E) (Supplementary fig. 2).

PCC-MRI: AVD reduced slightly at B (12.71%), without significant change at C (13.04%) (Fig. 1b). There was a dramatic increase in AVD at D (23.08%) that reduced greatly after the second stent placement, E (3.01%) (Table 1). aCSF velocity amplitude in the patient remained high at all time

points (table 2; supplementary fig. 2). Similarly, cCSF caudal peak velocity and flow remained constant all time points (table 2; supplementary fig. 2). Arterial flow showed a marked transient reduction after LP (8.45mL/s) (Fig. 2B). It returned to normal range values (13.55 ± 3.07mL/s) at C, D and E (13.44mL/s, 17.43mL/s and 15.11mL/s) (Table 1). Mean venous flow normalized at B (-8.32mL/s) but reduced to -5.47mL/s at C, improving again after stent placements to -10.47mL/s and -12.85mL/s. tIJV/tA improved markedly after LP to 98.41%, albeit transiently, since at C the percentage outflow reduced back to 40.74%. This percentage improved at D and E to reach 60.04% and 85.05% respectively (Table 1).

Discussion:

To our knowledge, this is the first study that describes simultaneous interactive changes in multiple fluid compartments of the brain and spine in a patient with IIH before and after medical and interventional therapies using a validated PCC-MR technique.

During systole, arterial pulsations in pial arterioles are transmitted directly into the incompressible CSF filled SAS. This transmitted pulse evokes a serious of events in the following temporal order: a) CSF in SAS shifts out of the foramen magnum; b) venous blood from the sinuses egresses out of the brain and c) part of the CSF from the ventricles is displaced out towards the spinal SAS (Ambarki *et al.*, 2007). During the diastolic phase, venous outflow decreases and venous blood is stored in the highly compliant thin-walled cortical and bridging veins that drain into the SSS (Bateman, 2003). An increase in SSS pressure would hamper venous outflow from cortical and bridging veins. In addition,

there will be increased collateral flow and increased mean transit time, that would redirect the volume of venous blood through a longer path within the cranial cavity (Mancini *et al.*, 2012). It is reasonable to suggest that this might result in a "permanent" increased volume of venous blood in the cranial cavity. Could this extra "stored" blood in the cortical veins be "tumoral"?

By applying Darcy's basic law of flow we can relate flow q (volume transferred per unit time) to pressure difference $\Delta p = p_u - p_d$ and resistance R, namely

$$q = \frac{\Delta p}{R}$$

Here p_u denotes upstream pressure and p_d denotes downstream pressure. We note that this law ignores the pulsatile, time dependent nature of flow and relies solely on averaged values. Bateman invoked this law to relate ICP to CSF outflow q_{CSF} , from the cerebral SAS into the superior sagittal sinus (SSS), and to pressure p_{SSS} in SSS as follows:

$$p_{SAS} = p_{SSS} + q_{CSF} R_{CSF}$$

with R_{CSF} denoting resistance to CSF outflow (Bateman, 2008a). Invoking again Darcy's law of flow, we can express the total cerebral venous outflow q_{CVO} from the brain into the right atrium as

$$q_{CVO} = \frac{p_{SSS} - p_{RA}}{R_{CVO}}$$

where p_{RA} is the pressure in the right atrium and R_{CVO} is the resistance to venous flow from the brain to the heart. We note that this is a very rough approximation to a very complex process but nonetheless gives some useful insight. By combining the last two equations and noting that ICP is accepted to be p_{SAS} we can express ICP as

$$IC\square = p_{RA} + q_{CSF}R_{CSF} + q_{CVO}R_{CVO}$$

In the event of an increase in the external pressure (ICP or p_{SAS}), assuming frozen values for the remaining values, the sinus wall will collapse and increase R_{CVO} and vice versa. Increased R_{CVO} can be reduced either indirectly by removing CSF through LP or CSF diversion procedures or directly by placing a venous sinus stent that will mechanically keep the vessels patent, facilitating venous outflow. The added benefit in the second case is an improvement in CSF reabsorption into SSS in addition to being a long term effect (Aguilar-Pérez *et al.*, 2017)

The most important complication, although rare, is remote or stent-adjacent stenosis (Raper *et al.*, 2017). Our patient developed a high-pressure difference in the right TS suggesting the presence of continued increased external CSF pressure. This underscores the importance of considering the entire cerebral venous system to avoid collapse of previously normal compliant veins (Bateman, 2008b).

PCC-MRI flow analysis in our patient provided us useful additional information regarding changes in fluid dynamics. Despite increased ICP, our results show that the overall fluid dynamics and temporal order of all fluid systolic peaks were normal before treatment (Fig. 1a), although AVD, AaCD and AcCD were slightly prolonged. We deduce that all fluid compartments respond physiologically, albeit with longer time delays. Medical treatment alone did not change these time delays, but both CSF removal and stent placements greatly enhanced the response of fluids to arterial input (Fig. 1). In addition, and most importantly, blood flow analysis shows that both CSF removal and venous

stenting greatly improves mean venous outflow. This data suggests that our patient had extrinsic reversible stenosis.

The dramatic reduction in the arterial flow profile after LP is curious and we do not have an explanation for this observation. However we conjecture that there might be a degree of arterial hyperemia in line with Bateman's observation regarding increased arterial inflow in IIH (Bateman, 2008b). By reducing R_{CVO} by CSF removal, a possible new setting of pressure changes and flow dynamics through cerebral autoregulatory mechanisms might in part explain such changes (Miller *et al*., 1972; Moriyasu and Hayashi, 1978).

The limitations of this study are linked to data derived from a single patient study. However, all variables in our patient were kept constant to monitor changes making comparisons easy. Since all interventions were intended for treatment, some results at later time points might reflect cumulative effects of previous treatments.

Conclusions

A thorough analysis of interactive intracranial fluid dynamics may provide the key in understanding what causes increased ICP in IIH and how best to treat it. Increased resistance to cerebral venous outflow may result in "storage" of extra intracranial venous volume. Venous stenting may be an efficacious strategy to improve egression of cerebral venous blood in the long-term.

Acknowledgements

The authors thank Prof. E. M. Haacke for providing us the software, Signal Processing in NMR, for CSF and flow analysis.

Abualenain J, Ranninger C, Jacobs D. Measurement of CSF opening pressure during lumbar puncture in the sitting position in the Emergency Department. academic emergency medicine 2011; Volume 18, Supplement 1: S4–S249.

Aguilar-Pérez M, Martinez-Moreno R, Kurre W, Wendl C, Bäzner H, Ganslandt O, et al. Endovascular treatment of idiopathic intracranial hypertension: retrospective analysis of immediate and long-term results in 51 patients. 2017: 1–11.

Ambarki K, Baledent O, Kongolo G, Bouzerar R, Fall S, Meyer M-E. A New Lumped-Parameter Model of Cerebrospinal Hydrodynamics During the Cardiac Cycle in Healthy Volunteers. IEEE Trans. Biomed. Eng. 2007; 54: 483–491.

Bateman GA. The reversibility of reduced cortical vein compliance in normal-pressure hydrocephalus following shunt insertion. Neuroradiology 2003; 45: 65–70.

Bateman GA. Stenoses in Idiopathic Intracranial Hypertension: To Stent or Not To Stent? AJNR Am J Neuroradiol 2008a; 29: 215–215.

Bateman GA. Arterial inflow and venous outflow in idiopathic intracranial hypertension associated with venous outflow stenoses. Journal of Clinical Neuroscience 2008b; 15: 402–408.

Beggs CB, Magnano C, Shepherd SJ, Marr K, Valnarov V, Hojnacki D, et al. Aqueductal cerebrospinal fluid pulsatility in healthy individuals is affected by impaired cerebral venous outflow. J. Magn. Reson. Imaging 2013; 40: 1215–1222.

Beggs CB. Cerebral venous outflow and cerebrospinal fluid dynamics. Veins and Lymphatics 2014; 3: 1–8.

Buell TJ, Raper DMS, Pomeraniec IJ, Ding D, Chen C-J, Taylor DG, et al. Transient resolution of venous sinus stenosis after high-volume lumbar puncture in a patient with idiopathic intracranial hypertension. J. Neurosurg. 2017: 1–4.

Doepp F, Schreiber SJ, Münster von T, Rademacher J, Klingebiel R, Valdueza JM. How does the blood leave the brain? A systematic ultrasound analysis of

cerebral venous drainage patterns. Neuroradiology 2004; 46: 565–570.

Enzmann DR, Pelc NJ. Cerebrospinal fluid flow measured by phase-contrast cine MR. AJNR Am J Neuroradiol 1993; 14: 1301–7– discussion 1309–10.

Farb NAS, Grady CL, Strother S, Tang-Wai DF, Masellis M, Black S, et al. Abnormal network connectivity in frontotemporal dementia: Evidence for prefrontal isolation. 2013; 49: 1856–1873.

Farb RI, Vanek I, Scott JN, Mikulis DJ, Willinsky RA, Tomlinson G, et al. Idiopathic intracranial hypertension: The prevalence and morphology of sinovenous stenosis. Neurology 2003; 60: 1418–1424.

Friedman DI, Liu GT, Digre KB. Revised diagnostic criteria for the pseudotumor cerebri syndrome in adults and children. Neurology 2013; 81: 1159–1165.

Juhász J, Lindner T, Jansen O, Margraf NG, Rohr A. Changes in intracranial venous hemodynamics in a patient with idiopathic intracranial hypertension after lumbar puncture precedes therapeutic success. J. Magn. Reson. Imaging 2017; 47: 286–288.

Kim DS, Choi JU, Huh R, Yun PH, Kim DI. Quantitative assessment of cerebrospinal fluid hydrodynamics using a phase-contrast cine MR image in hydrocephalus. Childs Nerv Syst 1999; 15: 461–467.

Lagana MM, Chaudhary A, Balagurunathan D, Utriainen D, Kokeny P, Feng W, et al. Cerebrospinal fluid flow dynamics in multiple sclerosis patients through phase contrast magnetic resonance imaging. Curr Neurovasc Res 2014; 11: 349–358.

Lagana MM, Shepherd SJ, Pietro Cecconi, Beggs CB. Intracranial volumetric changes govern cerebrospinal fluid flow in the Aqueduct of Sylvius in healthy adults. Biomedical Signal Processing and Control 2017; 36: 84–92.

Lee JH, Lee HK, Kim JK, Kim HJ, Park JK, Choi CG. CSF flow quantification of the cerebral aqueduct in normal volunteers using phase contrast cine MR imaging. Korean J Radiol 2004; 5: 81–86.

Mancini M, Morra VB, Di Donato O, Maglio V, Lanzillo R, Liuzzi R, et al. Multiple sclerosis: cerebral circulation time. Radiology 2012; 262: 947–955.

Miller JD, Stanek A, Langfitt TW. Concepts of Cerebral Perfusion Pressure and Vascular Compression During Intracranial Hypertension. In: Cerebral Blood Flow. Elsevier; 1972. p. 411–432.

Mollan SP, Ali F, Hassan-Smith G, Botfield H, Friedman DI, Sinclair AJ. Evolving evidence in adult idiopathic intracranial hypertension: pathophysiology and management. Journal of Neurology, Neurosurgery & Psychiatry 2016; 87: 982–992.

Moriyasu N, Hayashi N. [Concepts of cerebral perfusion pressure and venous outflow mechanism during intracranial hypertension (author's transl)]. Neurol.

Med. Chir. (Tokyo) 1978; 18: 1–10.

Morris PP, Black DF, Port J, Campeau N. Transverse Sinus Stenosis Is the Most Sensitive MR Imaging Correlate of Idiopathic Intracranial Hypertension. AJNR Am J Neuroradiol 2017; 38: 471–477.

Passi N, Degnan AJ, Levy LM. MR Imaging of Papilledema and Visual Pathways: Effects of Increased Intracranial Pressure and Pathophysiologic Mechanisms. AJNR Am J Neuroradiol 2013; 34: 919–924.

Raper DMS, Buell TJ, Ding D, Pomeraniec IJ, Crowley RW, Liu KC. A pilot study and novel angiographic classification for superior sagittal sinus stenting in patients with non-thrombotic intracranial venous occlusive disease. J NeuroIntervent Surg 2017: neurintsurg–2016–012906–5.

Rohr A, Dörner L, Stingele R, Buhl R, Alfke K, Jansen O. Reversibility of venous sinus obstruction in idiopathic intracranial hypertension. AJNR Am J Neuroradiol 2007; 28: 656–659.

Shang H, Liu H, Yan L, Lei J, Cui C, Li H. Quantitative assessment of physiological cerebrospinal fluid flow in the cervical spinal canal with 3.0T phase-contrast cine MRI. Neural Regen Res 2012; 7: 1392–1397.

Stoquart-El Sankari S, Lehmann P, Gondry-Jouet C, Fichten A, Godefroy O, Meyer ME, et al. Phase-Contrast MR Imaging Support for the Diagnosis of Aqueductal Stenosis. American Journal of Neuroradiology 2008; 30: 209–214.

Sundström P, Wåhlin A, Ambarki K, Birgander R, Eklund A, Malm J. Venous and cerebrospinal fluid flow in multiple sclerosis: A case-control study. Ann Neurol. 2010; 68: 255–259.

Yousef MI, Mageed El AEA, Yassin AEN, Shaaban MH. Use of cerebrospinal fluid flow rates measured by phase-contrast MR to differentiate normal pressure hydrocephalus from involutional brain changes. The Egyptian Journal of Radiology and Nuclear Medicine 2016; 47: 999–1008.

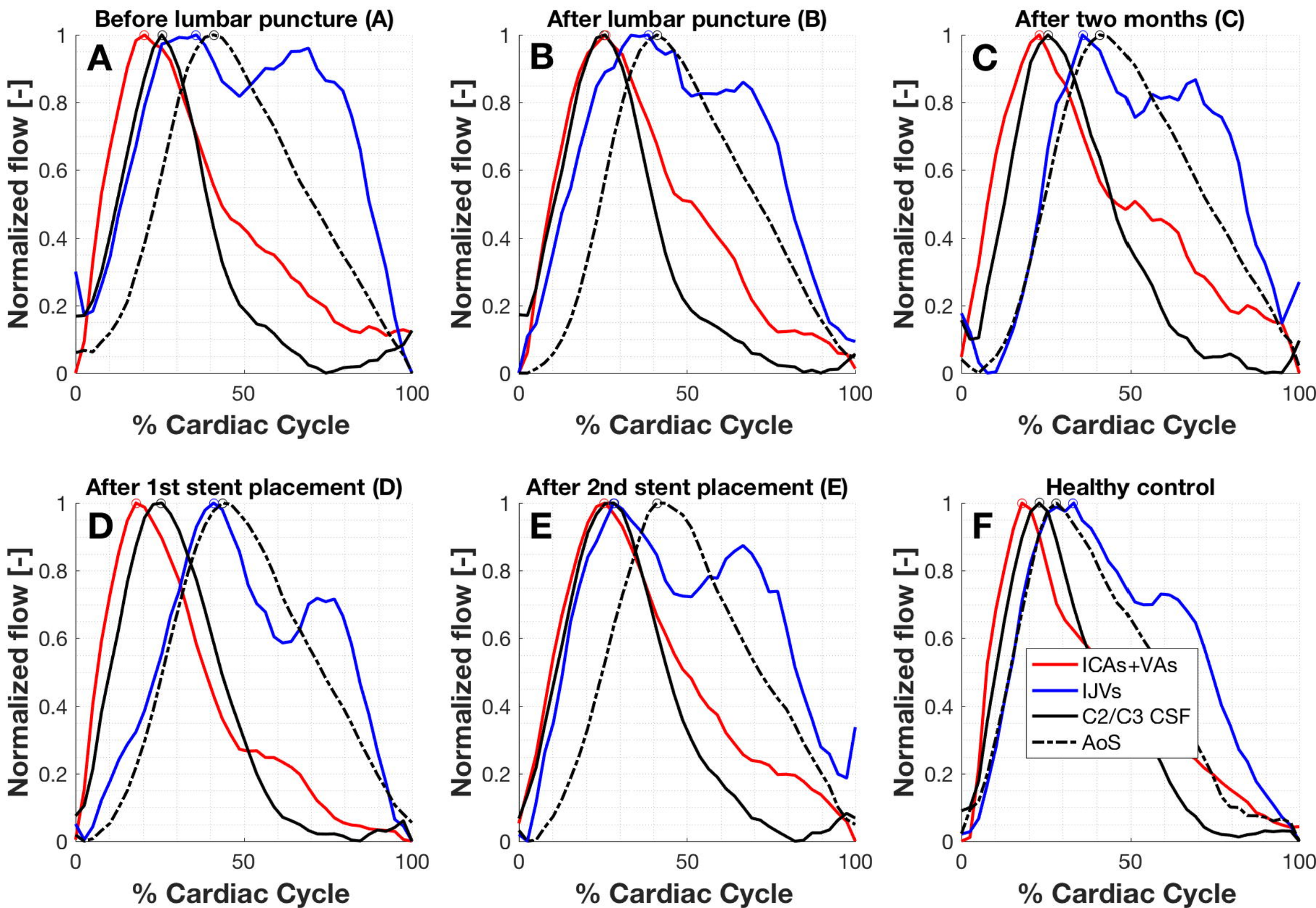
Before lumbar puncture (A)
A
After lumbar puncture (B)
B
After two months (C)
C
After 1st stent placement (D)
D
After 2nd stent placement (E)
E
Healthy control
F
Normalized flow [-]
% Cardiac Cycle
0
0.2
0.4
0.6
0.8
1
0
50
100
ICAs+VAs
IJVs
C2/C3 CSF
AoS

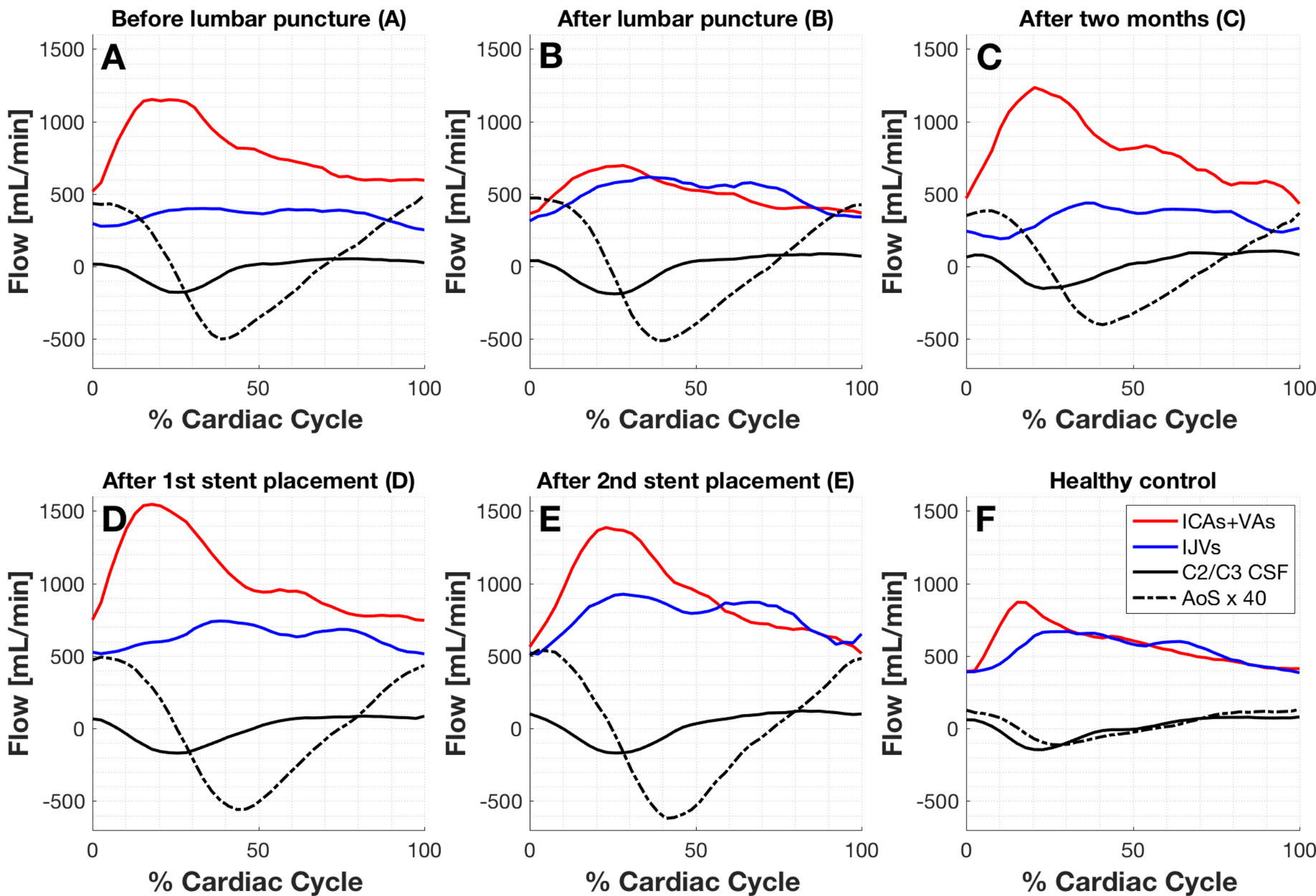
Before lumbar puncture (A)
After lumbar puncture (B)
After two months (C)
After 1st stent placement (D)
After 2nd stent placement (E)
Healthy control
A
B
C
D
E
F
Flow [mL/min]
% Cardiac Cycle
1500
1000
500
0
-500
0
50
100
ICAs+VAs
IJVs
C2/C3 CSF
AoS x 40

	Mean flow (mL/s)	**Systolic peak (mL/s)**	**Diastolic peak (mL/s)**	**|tIJV/tA| %**	**AV delay %CC**
Arterial flow (ICAs+VAs)					
Before lumbar puncture (A)	13.35	19.19	9.67	44.05	-
After lumbar puncture (B)	8.45	11.61	6.28	98.41	-
Before two months (C)	13.44	20.56	8.37	40.74	-
After 1st stent placement (D)	17.43	25.75	12.69	60.04	-
After 2nd stent placement (E)	15.11	23.09	9.44	85.05	-
Healthy control	9.59	14.51	6.79	93.51	-
Normal range	13.55±3.07	18.13±2.55	7.67±1.65	71.1±22	-
Reference	(Sundström *et al.*, 2010)	(Stoquart-El Sankari *et al.*, 2008)	(Stoquart-El Sankari *et al.*, 2008)	(Lagana *et al.*, 2014)	-
Venous flow (IJVs)					
Before lumbar puncture (A)	-5.88	-6.66	-4.45	-	15.38
After lumbar puncture (B)	-8.32	-10.28	-5.58	-	12.71
Before two months (C)	-5.47	-7.30	-3.19	-	13.04
After 1st stent placement (D)	-10.47	-12.35	-8.52	-	23.08
After 2nd stent placement (E)	-12.85	-15.43	-9.08	-	3.01
Healthy control	-8.98	-11.13	-6.53	-	15.05
Normal range	-9.42±2.37	-10.93±5.71	-5.62±1.80	-	12.5±8.06
Reference	(Sundström *et al.*, 2010)	(Stoquart-El Sankari *et al.*, 2008)	(Stoquart-El Sankari *et al.*, 2008)	-	(Ambarki *et al.*, 2007)

	Mean flow (mL/s)	**Caudal peak flow (mL/s)**	**Diastolic peak flow(mL/s)**	**Caudal peak velocity (cm/s)**	**Cranial peak velocity (cm/s)**	**Velocity pulsatility (cm/s)**	**Arterio-CSF delay %CC**
C2-C3 CSF							
Before lumbar puncture (A)	-0.26	-2.96	0.90	-2.93	0.89	3.82	5.35
After lumbar puncture (B)	-0.02	-3.14	1.48	-3.11	1.46	4.57	-0.33
Before two months (C)	0.29	-2.50	1.77	-2.50	1.77	4.27	2.68
After 1st stent placement (D)	-0.02	-2.82	1.43	-2.79	1.41	4.21	7.36
After 2nd stent placement (E)	0.29	-2.81	2.04	-2.78	2.02	4.80	2.68
Healthy control	0.09	-2.43	1.30	-2.08	1.11	3.19	5.02
Normal range	0.08±1.33	-3.27±0.70	1.69±0.50	-2.05±1.31	1.10±1.12	-	5.35±2.36
Reference	(Lagana *et al.*, 2017)	(Stoquart-El Sankari *et al.*, 2008)	(Lagana *et al.*, 2014)	(Shang *et al.*, 2012)	(Shang *et al.*, 2012)	-	(Ambarki *et al.*, 2007)
Aqueduct of Sylvius							
Before lumbar puncture (A)	0.02	-0.28	0.25	-6.47	5.77	12.24	20.74
After lumbar puncture (B)	0.01	-0.28	0.26	-6.60	5.95	12.55	15.38
Before two months (C)	0.01	-0.22	0.21	-5.18	4.97	10.15	18.06
After 1st stent placement (D)	0.00	-0.31	0.27	-7.22	6.26	13.48	25.75
After 2nd stent placement (E)	0.00	-0.34	0.30	-8.01	6.92	14.93	15.72
Healthy control	0.01	-0.06	0.07	-2.01	2.15	4.15	10.03
Normal range	0.03±0.013	-0.10±0.06	0.10±0.05	3.65±1.59	2.60±1.45	-	22.1±74.66
Reference	(Lee *et al.*, 2004)	(Lagana *et al.*, 2017)	(Lagana *et al.*, 2017)	(Lee *et al.*, 2004)	(Kim *et al.*, 1999)	-	(Ambarki *et al.*, 2007)